



**HAL**  
open science

## Characterization of At- species in simple and biological media by high performance anion exchange chromatography coupled to gamma detector.

A. Sabatié-Gogova, Julie Champion, Sandrine Huclier, Nathalie Michel, F. Pottier, N. Galland, Z. Asfari, M. Chérel, Gilles F Montavon

### ► To cite this version:

A. Sabatié-Gogova, Julie Champion, Sandrine Huclier, Nathalie Michel, F. Pottier, et al.. Characterization of At- species in simple and biological media by high performance anion exchange chromatography coupled to gamma detector.. *Analytica Chimica Acta*, 2012, 721, pp.182. 10.1016/j.aca.2012.01.052 . in2p3-00681129

**HAL Id: in2p3-00681129**

**<https://in2p3.hal.science/in2p3-00681129v1>**

Submitted on 20 Mar 2012

**HAL** is a multi-disciplinary open access archive for the deposit and dissemination of scientific research documents, whether they are published or not. The documents may come from teaching and research institutions in France or abroad, or from public or private research centers.

L'archive ouverte pluridisciplinaire **HAL**, est destinée au dépôt et à la diffusion de documents scientifiques de niveau recherche, publiés ou non, émanant des établissements d'enseignement et de recherche français ou étrangers, des laboratoires publics ou privés.

1 **Characterization of At<sup>-</sup> species in simple and biological media by high performance**  
2 **anion exchange chromatography coupled to gamma detector.**

3

4

5 A. Sabatié-Gogova<sup>a</sup>, J. Champion<sup>a</sup>, S. Huclier<sup>a</sup>, N. Michel<sup>a</sup>, F. Pottier<sup>a</sup>, N. Galland<sup>b</sup>, Z.  
6 Asfari<sup>c</sup>, M. Chérel<sup>d</sup>, G. Montavon<sup>a\*</sup>

7

8

9 <sup>a</sup> Laboratoire SUBATECH, UMR CNRS 6457 IN2P3 Ecole des Mines de Nantes, 4 rue A.  
10 Kastler, 44307 Nantes Cedex, France. [sabatie@subatech.in2p3.fr](mailto:sabatie@subatech.in2p3.fr),  
11 [champion@subatech.in2p3.fr](mailto:champion@subatech.in2p3.fr), [pottier@subatech.in2p3.fr](mailto:pottier@subatech.in2p3.fr), [ledu@subatech.in2p3.fr](mailto:ledu@subatech.in2p3.fr),  
12 [huclier@subatech.in2p3.fr](mailto:huclier@subatech.in2p3.fr), [michel@subatech.in2p3.fr](mailto:michel@subatech.in2p3.fr)

13 <sup>b</sup> Laboratoire CEISAM, UMR CNRS 6230, Université de Nantes, 2 rue de la Houssinière,  
14 44322 Nantes Cedex, France. [nicolas.galland@univ-nantes.fr](mailto:nicolas.galland@univ-nantes.fr)

15 <sup>c</sup> IPHC, UMR CNRS 7178 IN2P3 ECPM, 25 rue Becquerel, 67087 Strasbourg Cedex, France.  
16 [asfariz@ecpm.u-strasbg.fr](mailto:asfariz@ecpm.u-strasbg.fr)

17 <sup>d</sup> IRT UN INSERM 892 CRCNA, Université de Nantes, 8 quai Moncoussu 44093, Nantes  
18 Cedex, France. [Michel.Cherel@univ-nantes.fr](mailto:Michel.Cherel@univ-nantes.fr)

19

20

21 **Keywords:** Astatine, speciation, ion-exchange, human serum

22

23 **Abstract**

24

25       Astatine is a rare radioelement belonging to the halogen group. Considering the trace  
26 amounts of astatine produced in cyclotrons, its chemistry cannot be evaluated by  
27 spectroscopic tools. Analytical tools, provided that they are coupled with a radioactive  
28 detection system, may be an alternative way to study its chemistry. In this research work,  
29 High Performance Anion Exchange Chromatography (HPAEC) coupled to a gamma detector  
30 ( $\gamma$ ) was used to evaluate astatine species under reducing conditions. Also, to strengthen the  
31 reliability of the experiments, a quantitative analysis using a reactive transport model has been  
32 done. The results confirm the existence of one species bearing one negative charge in the pH  
33 range 2–7.5. With respect to the other halogens, its behavior indicates the existence of  
34 negative ion, astatide  $\text{At}^-$ . The methodology was successfully applied to the speciation of the  
35 astatine in human serum. Under fixed experimental conditions (pH 7.4–7.5 and redox  
36 potential of 250 mV) astatine exists mainly as astatide  $\text{At}^-$  and does not interact with the major  
37 serum components. Also, the method might be useful for the *in vitro* stability assessment of  
38  $^{211}\text{At}$ -labelled molecules potentially applicable in nuclear medicine.  
39

40

## 41 1. INTRODUCTION

42

43

44 Astatine (At), element 85, is below iodine in the periodic table of elements. It is a rare  
45 element representing short half-life radioactive isotopes that have to be produced in  
46 cyclotrons [1].

47  $^{211}\text{At}$  is of considerable interest as it is a promising radiotherapeutic agent for targeted  
48 alpha therapy (TAT) in nuclear medicine [2-4]. In this field, the astatination through diazo  
49 intermediates under non-oxidizing mild conditions has been suggested to react with astatine  
50 anionic or radical species [5, 6]. The general approach developed more recently has been the  
51 use of bifunctional reagents conjugated to the proteins and labelled, similarly to the  
52 radioiodination, under oxidizing conditions of Chloramine T, hydrogen peroxide or N-  
53 iodosuccinimide with astatine cationic reactive species [2-7].

54 Astatinated molecules as well the bio-conjugates are quite unstable in vivo relative to their  
55 radioiodinated analogues [7]. Due to the fact that released astatine localizes in thyroid in  
56 humans, as iodide, iodate, chlorate, or pertechnetate [5] the form of astatide ( $\text{At}^-$ ) has been  
57 proposed. Furthermore, the distribution (in PBS) between plasma and blood cells in vitro has  
58 established that it is poorly entrapped within the erythrocytes, which render it available for the  
59 transport in the blood [8]. The mechanism of “deastatination” in vivo remains still unknown,  
60 Wilbur has only pointed out the complex character of probably enzymatic, biochemical and/or  
61 physical process [7]. The stability is generally assessed using in vitro studies with blood  
62 serum by thin layer chromatography. Although the method is rapid, it gives no indication  
63 about astatine speciation.

64 Astatine chemistry remains generally not well understood. It is an invisible element: the  
65 produced amount of astatine allows only ultra trace concentrations (typically  $10^{-11}$  to  $10^{-15}$   
66  $\text{mol L}^{-1}$ ) and thus no spectroscopic tools can be used to investigate astatine chemistry at the  
67 molecular level. In reducing conditions, astatine presents some other similarities with respect  
68 to its homologues of the halogen group, especially iodine. For example, it coprecipitates with  
69 insoluble iodide compounds [9,10] and astatine forms the hydrogen astatide (HAt) alike the  
70 halogens form hydrogen halides. The identification of  $\text{HAt}^+$  and  $\text{HI}^+$  species in gas phase by  
71 mass spectrometry [11] may be an indirect proof of the presence of  $\text{At}^-$ . Astatide ( $\text{At}^-$ ) is  
72 therefore an expected species in various media. Surprisingly, only a few people have  
73 endeavored to identify the astatide by means of analytical tools. The negative charge of  
74 astatine species has been deduced from its ability to be retained by anionic exchanger Aminex  
75 A27 [12-14], and from electromobility measurements [15]. Berei et al. [5], using the data of  
76 Roessler [14] from high-pressure liquid radiochromatography experiments, showed a linear  
77 correlation between the retention volume and the inverse ionic radius for halogens and  
78 concluded that the astatine species under study behave as halogenide  $\text{At}^-$ . However, as it will  
79 be discussed later, due to the proportionality of the retention volume to the selectivity  
80 coefficient, the correlation should show an exponential curve trend. This discrepancy makes  
81 the results of Roessler et al. questionable and new data are needed.

82 In this paper, the first objective is to acquire new data by high-performance anion-  
83 exchange chromatography under reducing conditions using simple media  $0.01\text{--}0.10 \text{ mol L}^{-1}$   
84  $\text{H}/\text{NaCl}$  (chloride as the exchange species) with pH values ranging from 2.0 to 7.5 for a better  
85 identification of astatine species. For comparison, experiments are also performed with other  
86 halogens anions ( $\text{F}^-$ ,  $\text{Br}^-$ ,  $\text{I}^-$ ). To help the evaluation of experimental data, a quantitative  
87 analysis using the reactive transport code PHREEQC [16] is proposed. Then, the second  
88 objective is to apply the methodology for speciation of astatine in blood serum. At pH of 7.4

89 its potential varies between 200 and 300 mV versus NHE (Normal Hydrogen Electrode) [17]  
90 which coincide with the values related to the existence of thermodynamically stable anionic  
91 astatine species.

92

93

## 94 **2. EXPERIMENTAL**

95

96

### 97 *2.1. Materials*

98

99

100 Commercially available chemical products of analytical grade or superior were purchased  
101 from Sigma-Aldrich. Transferrin from human blood plasma ( $\geq 95\%$ ) and albumin from  
102 human blood plasma ( $\geq 99\%$ ) were also purchased from Sigma-Aldrich. Human serum was  
103 supplied by Lonza.

104  $^{211}\text{At}$  was produced by the nuclear reaction  $^{209}\text{Bi}(\alpha, 2n)^{211}\text{At}$  at the CEMTHI cyclotron  
105 (Orléans, France). Bismuth (Bi) target was prepared by the evaporation of bismuth under  
106 vacuum onto nitride aluminium backing (shapal-M from Goodfellow). The ceramic backing  
107 has good thermal properties and is heat resistant under beam. An elliptical deposit with a  
108 surface area of  $3\text{ cm}^2$  and a homogeneous thickness between 22.3 and 30.0  $\mu\text{m}$  was obtained  
109 within few hours. The homogeneity of the deposit was checked using a profilometric analysis.  
110 Run duration as well as beam intensity were adapted to reach needed  $^{211}\text{At}$  activity. For the  
111 present work, duration run varied from 2 to 3 hours and beam intensity from 1.7 to 2.3  $\mu\text{A}$   
112 leading to production from 100 to 317 MBq at the end of bombardment.

113 Detailed information about the production can be found elsewhere [18,19]. Astatine from  
114 the target was recovered by dry distillation and captured in methanol (yield at about 80%)  
115 [19]. The radionuclide purity was monitored using  $\gamma$ -ray spectroscopy. In order to lower the  
116 X-ray contribution, a lead shielding was placed between the detector and the sample.  
117 Typically, the stock solutions were obtained with a specific activity close to 100 MBq mL<sup>-1</sup>.  
118 The radiotracer <sup>131</sup>I was obtained diluted in water with a specific activity close to 0.1MBq  
119 mL<sup>-1</sup> from the CHU Nuclear Medicine (Nantes, France).

120

121

## 122 2.2. *Analytical tools*

123

124

125 The radionuclidic purity of <sup>211</sup>At was monitored by  $\gamma$ -ray spectrometry with a high purity  
126 germanium (HPGe) detector. The activity of the stock astatine solution was measured on both  
127 the X-rays from <sup>211</sup>Po and <sup>211</sup>At and  $\gamma$ -rays at 687.00 keV from <sup>211</sup>At, using a suitable  
128 geometry previously calibrated with standard gamma sources. <sup>211</sup>At recovery after the  
129 HPAEC- $\gamma$  measurements was quantified by liquid scintillation counting using a Packard 2550  
130 TR/AB liquid scintillation analyzer with the Ultima Gold LLT scintillation liquid.

131 A Fisherbrand type electrode freshly calibrated against dilute standard pH buffers (pH 1–  
132 10, Merck) was used to determine the pH. The potential (E) of aqueous solutions was  
133 measured using a Pt combined redox electrode (Metrohm type) calibrated against the redox  
134 buffer (Fe(SCN)<sub>6</sub><sup>-3</sup>/Fe(SCN)<sub>6</sub><sup>-4</sup>, 215 mV/Pt/SCE, Radiometer Analytical).

135 The HPLC device is a Dionex UltiMate3000 system consisting of a DGP-3600 MB pump,  
136 an AS3000 auto-sampler, a TCC-3200B column oven and a diode array DAD-3000 detector.  
137 The stationary phase is a Dionex AS20 anionic exchange column (0.2 cm diameter x 25 cm

138 length), with an AG20 guard column (0.2 cm diameter × 5 cm length). The AS20 consists of a  
139 hydrophilic polymer grafted with quaternary alkanol ammonium. The total capacity  
140 represented by both columns is 0.079 milliequivalents (meq). The degree of Cross-Linking (%  
141 of DiVinylBenzene, %DVB) amounts to 55%. The resin was designed for working in NaOH  
142 or KOH media. However, taking into account the context of the study, the sodium chloride  
143 medium was chosen (see 2.3. Experimental procedure). The  $\gamma$ -ray detector is a Raytest  
144 GabiStar, piloted by Gina Software. Count rate is 0–500.000 cps. The detection energy  
145 window was set between 50 and 1630 keV. Experimental data were acquired and processed  
146 by Chromeleon 6.80 Chromatograph Software.

147 The components in stock solutions and collected fractions were quantified by Inductively  
148 coupled plasma mass spectrometry (ICPMS) XSERIES2 Thermo Scientific for I<sup>-</sup>, by Ion  
149 Chromatography (IC) with conductivity detection ICS 2500 from Dionex for F<sup>-</sup> and Br<sup>-</sup>, and  
150 by UV–VIS Spectrophotometer UV-1800 Shimadzu for albumin and transferrin by using the  
151 absorption coefficients of  $9.30 \times 10^4$  and  $3.53 \times 10^4$  cm<sup>-1</sup> mol<sup>-1</sup> L at 280 nm, respectively [20].

152

153

### 154 2.3. *Experimental procedures*

155

156

157 The solutions and eluents were freshly prepared using degassed (by ultrasonics) Milli-Q  
158 deionized water under argon atmosphere. Astatine is a redox-sensitive species [21]. In all  
159 eluents, the redox couple SO<sub>3</sub><sup>2-</sup>/S<sub>2</sub>O<sub>3</sub><sup>2-</sup> (10<sup>-4</sup>/10<sup>-3</sup> mol L<sup>-1</sup>) was used to maintain the potential at  
160 250 mV versus NHE (Normal Hydrogen Electrode). It is a mean value characterizing the  
161 serum potential which varies between 200 and 300 mV versus NHE [17]. For astatine-in-  
162 blood serum assays, the eluent composition was close to the physiological solution (10<sup>-1</sup> mol



163 L<sup>-1</sup> NaCl, pH 7.4). The pH was buffered with 10<sup>-3</sup> mol L<sup>-1</sup> PBS that, as 10-fold concentrate,  
164 contains 10<sup>-1</sup> mol L<sup>-1</sup> of sodium phosphate (Na<sub>3</sub>PO<sub>4</sub>) and 9% of NaCl. For the other  
165 experiments, 10<sup>-1</sup> mol L<sup>-1</sup> NaCl (with or without 10<sup>-2</sup> mol L<sup>-1</sup> HCl) was used unless otherwise  
166 stated. Eluents were kept under argon flow during proceedings.

167 The stock solutions were prepared by dissolving the appropriate mass of NaX (X = F, Cl,  
168 Br, I) salts and each protein (not purified) in eluent under argon atmosphere. The samples (10<sup>-4</sup>,  
169 10<sup>-5</sup> and 10<sup>-6</sup> mol L<sup>-1</sup> of NaX, 4.6 10<sup>-6</sup> mol L<sup>-1</sup> of transferrin and 7.9 10<sup>-5</sup> mol L<sup>-1</sup> of albumin)  
170 were prepared by dilution in the appropriate eluent. pH was set to 2 by adding the appropriate  
171 volume of HCl to some samples of NaX. The commercial serum was three times diluted in  
172 the physiological-type eluent. The <sup>211</sup>At stock solution in methanol was added to the solutions  
173 with varying concentrations from 6 10<sup>-14</sup> to 1.5 10<sup>-11</sup> mol L<sup>-1</sup>. The mixtures were agitated for 2  
174 h at 25 °C for equilibration.

175 The HPAEC method included a cleaning step by elution with HCl, the pH shifting  
176 gradually from 5 to 2 during 20 min, followed by checking the resin stability. This was done  
177 using I<sup>-</sup> (10<sup>-5</sup> mol L<sup>-1</sup>) as internal standard giving a retention time of 11.2 min for a new AS20  
178 column using 10<sup>-1</sup> mol L<sup>-1</sup> NaCl at 350 μL min<sup>-1</sup>. Over time, the shift of 0.6 min towards  
179 lower retention time was observed which is explained by a small decrease of the site capacity  
180 of the resin and was taken into account in the quantitative modeling (see 3. Results and  
181 discussion). Finally, the system was pre-equilibrated with the eluent of interest. The pre-  
182 equilibration was controlled by measurement of pH and E at the inlet of the column and the  
183 outlet of gamma detector. All experiments were performed under isocratic conditions at 25  
184 °C. Samples were injected into the column through a 50 μL sample loop injector. I<sup>-</sup> and Br<sup>-</sup>  
185 (both 10<sup>-5</sup> mol L<sup>-1</sup>) were detected online spectrophotometrically at 230, 214 nm, proteins and  
186 blood serum at 280 nm. An online detection of astatine was done by γ-ray detector. F<sup>-</sup> (5x10<sup>-5</sup>  
187 mol L<sup>-1</sup>) was detected offline (from collected fractions) by IC with conductivity detection.

188 The recovery was determined from measurement of species' concentration before injection  
189 and in the collected fractions.

190 For clarity in the data interpretation, the results are exploited as retention factors (k) with:

$$191 \quad k = \frac{t_R - t_D}{t_D} \quad (1)$$

192  $t_R$  and  $t_D$  being the retention time and the dead time (corresponding to the method of detection  
193 used), respectively. When retention times are given, they refer to the position on the UV  
194 chromatogram.

195

196

#### 197 2.4. *Quantitative analysis of experimental data*

198

199

200 PHREEQC is a 1D transport code [16] built for transport processes modeling including  
201 diffusion, advection and dispersion. All of these processes are combined with equilibrium and  
202 kinetic chemical reactions. Initially developed for modeling the transport of contaminants in  
203 soils, it is also well suited for the modeling of liquid chromatography data because the  
204 processes in analytical and environmental fields are likely identical. The input file, divided  
205 into three blocks, is briefly explained as follow.

206 The first block involves the aqueous speciation calculations. Using a chemical  
207 composition of each solution (potential, pH, solutes and concentrations), it calculates the  
208 distribution of aqueous species using implemented thermodynamic databases. In the current  
209 study, the LLNL (Lawrence Livermore National Laboratory) thermodynamic database for F,  
210 Cl, Br and I, and the recently reported data for At [21], were used for the modeling. All  
211 equilibrium constants were extrapolated at zero ionic strength using the Truncated Davies  
212 equation [22].

213 The second block involves the transport. As it will be experimentally shown latter, the  
 214 transport is imposed by the high pressure pump and can be considered as an advection  
 215 process. The diffusion process, which affects the width of the elution peaks, was not  
 216 considered since the paper is interested in the retention properties of the exchanger.

217 The third block describes the reaction at the surface of the exchanger. Ion-exchange being  
 218 an important mechanism occurring in soils, it is implemented in the code through the Gaines-  
 219 Thomas convention [23] which was used in the study. The approach uses the law of mass  
 220 action, based on half-reactions between an aqueous species and a fictive unoccupied exchange  
 221 site for each exchanger. The reaction for the exchange species S-Cl is:



223 where  $\text{S}^+$  represents the exchange master species. Since all exchange sites are filled by  
 224 exchange species (the concentration of master species is forced to zero), the master species is  
 225 not included in the mole-balance equation for the exchanger. The activities of the exchange  
 226 species are defined as equivalent fractions, being equal to the moles of sites occupied by an  
 227 exchange species divided by the total number of exchange sites, in equivalents per L of  
 228 solution (when density = 1). In NaCl medium, the exchange reaction of  $\text{X}^-$  ( $\text{X} = \text{F}, \text{Br}, \text{I}$  and  
 229  $\text{At}$ ) can be written as:



231 The distribution of species is given by the law of mass action:

$$232 \quad K_{X/Cl} = \frac{\{S-X\}\{Cl^-\}}{\{X^-\}\{S-Cl\}} = \frac{K_x}{K_{Cl}} \quad (4)$$

233 Curly brackets indicate the activities, and  $K_x$  and  $K_{Cl}$  the coefficients describing the  
 234 interaction between the specified anion  $\text{X}^-$  and the exchange site  $\text{S}^+$  according to the equation  
 235 (2). The exchange or selectivity coefficients  $K_{X/Cl}$  given in the paper are relative to  $\text{Cl}^-$ , i.e.  
 236  $K_{Cl/Cl} = 1$ . The activity coefficient for an exchange species is known to strongly depend on the

237 exchanger composition and the ionic strength [24, 25]. In the present study, the exchange  
 238 species corresponds to S-Cl and the ionic strength is fixed to  $10^{-1}$  mol L<sup>-1</sup>. We then fix the  
 239 activity coefficient constants equal to 1.

240

241

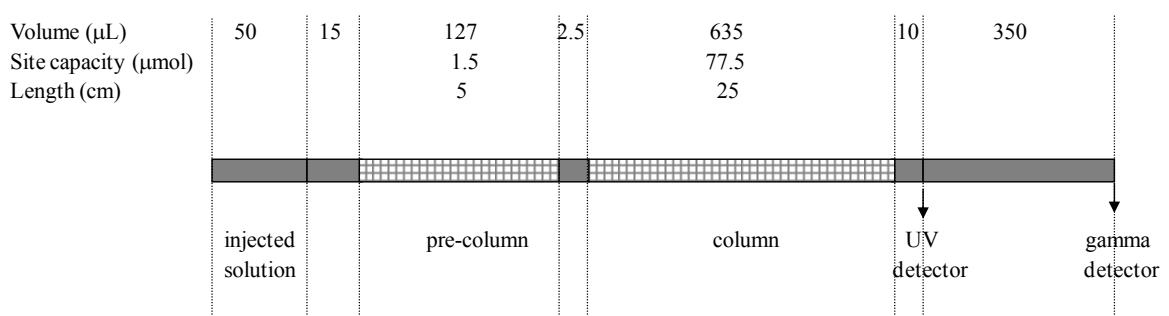
## 242 2.5. Model development

243

244

245 The system represented by the injection loop, tubing and columns is decomposed into a  
 246 number of cells. Each cell is characterized by a given volume of water (whose composition is  
 247 defined) and a given height. This simplistic representation of the system, the characteristics of  
 248 which are given by DIONEX, is shown in Fig. 1. The model describes the void volume of a  
 249 non-sorbing species, which corresponds to an UV peak at 2.4 min for a flux of 350  $\mu\text{L min}^{-1}$ .  
 250 The difference in volume (350  $\mu\text{L}$ ) between the two detectors was experimentally determined  
 251 using both stable (<sup>127</sup>I) and radioactive (<sup>131</sup>I) iodide.

252 Fig. 1.



253

254 According to the ion-exchange reaction, sites (in mol) are added into the cells associated  
 255 to the exchanger. For each cell, the initial conditions and the set of reactants can be defined  
 256 individually, which provides flexibility to simulate a variety of chemical conditions  
 257 throughout the column. It is then possible to differentiate between the pre-column, the AG20

258 guard column being packed with a resin of proportionally lower capacity, and the column  
259 AS20. Nevertheless, in the model, it was assumed that the selectivity coefficients are identical  
260 in both columns. Also, it was calculated that the guard column placed on-line prior to the  
261 analytical column increases retention time of about 4%. This value is in good agreement with  
262 supplier's information.

263 The infilling solution for the column is always solution number 0. Advection is modeled  
264 by "shifting" the solution 0 to cell 1, the solution in cell 1 to cell 2, and so on. At each shift,  
265 equilibrium is maintained in each cell.

266 The model was first tested with trace amount of iodide ( $10^{-4}$  mol L<sup>-1</sup>) in  $3.5 \times 10^{-1}$  mol L<sup>-1</sup>  
267 NaOH medium. The experimental result has led to a retention factor  $k_I$  of 2.3. In such simple  
268 conditions (analyte occupies <1% of the column capacity, exchange between two monovalent  
269 anions), the exchange coefficient can be simply calculated according to:

$$270 \quad K_{OH/I} = \frac{Q}{V_m \{OH^{-}\}} \frac{1}{k_I} \quad (5)$$

271 where  $Q$  is the capacity of the column in meq, and  $V_m$  is the dead volume of the column in  
272 mL. A value of 1.19 can be calculated (with  $K_{OH/OH} = 1$ ) and agrees with the one derived from  
273 PHREEQC. The input file used for the calculation is given in the supplementary information.

274

275

### 276 3. RESULTS AND DISCUSSION

277

278

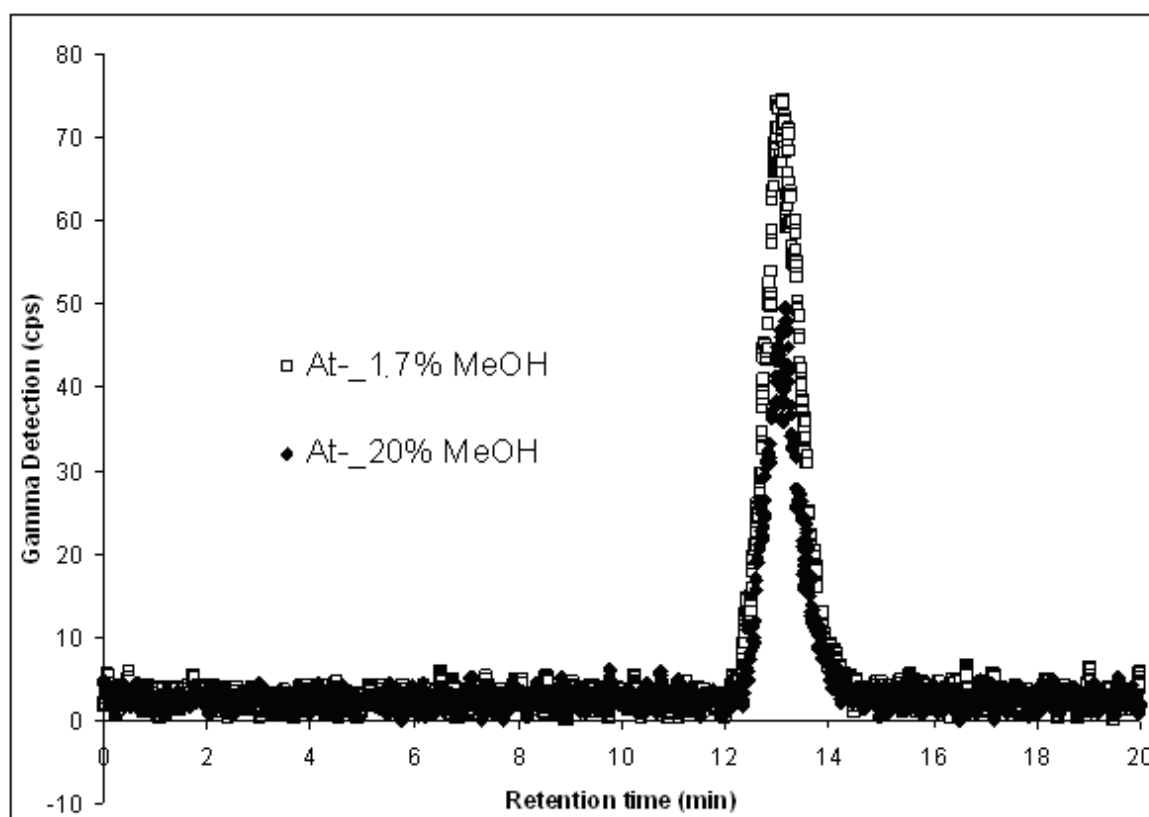
#### 279 3.1. Characterization of *At*

280

281

282 A typical gamma chromatogram is presented in Fig. 2. It shows a significant retention of  
283 astatine species on the anion exchanger with the retention time of 13 min and a recovery yield  
284 between 70 and 100%. It has been also settled that the retention of the astatine species is not  
285 affected by the presence of methanol coming from astatine stock solutions. In a typical  
286 experiment, the methanol content amounts to 2–5%. When varying the content of methanol  
287 from 1 even to 20% (in volume), no significant peak shift has been observed. This retention  
288 did not prove that an anionic species exists and the exchange reaction has occurred. In a  
289 recent work [26], some of us have shown that the cationic species of astatine existing under  
290 acidic oxidizing conditions can be adsorbed on both anionic and cationic exchangers. This  
291 peculiar behavior is related to the ultra-traces concentrations of astatine used in the  
292 experiments.

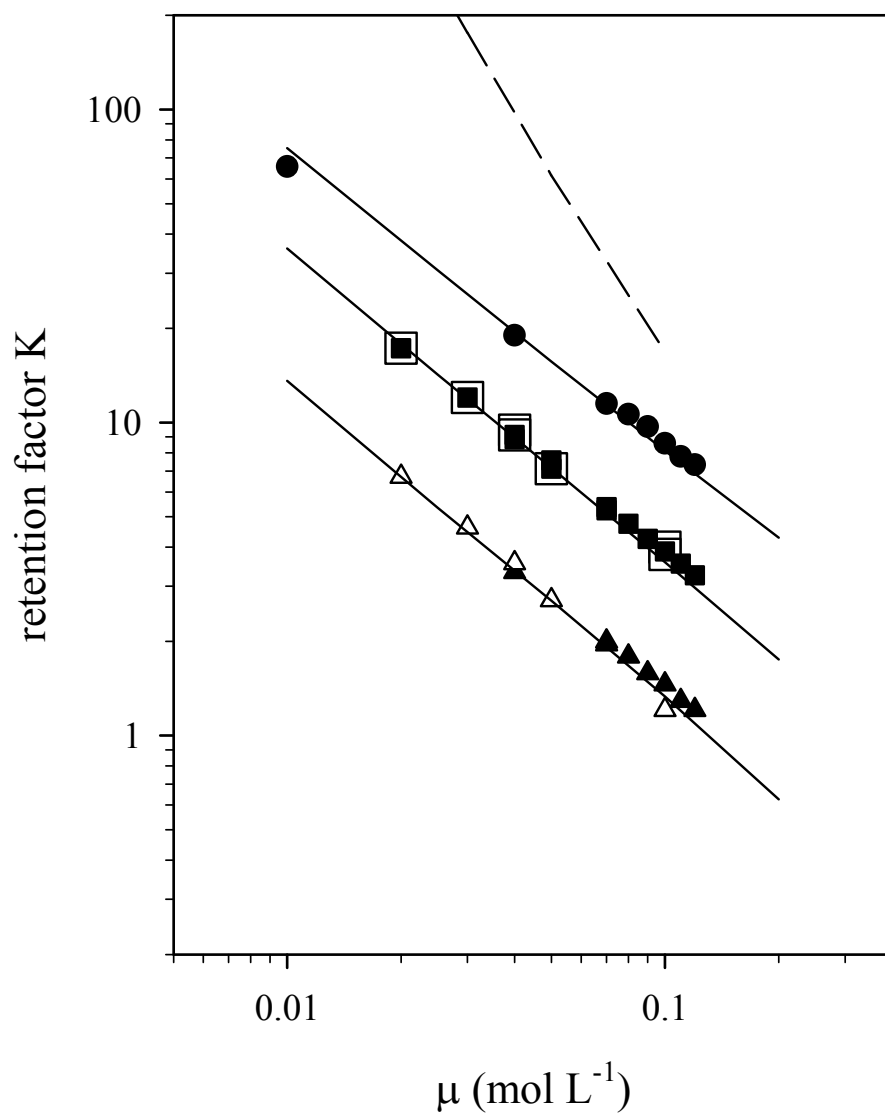
293 Fig. 2.



294

295 The quantitative analysis of further experimental data based on equation (3) has been  
296 done. The competition effects for exchange sites were considered between chloride and  
297 medium anions including astatine species. The competition with the hydroxide and the redox  
298 couple  $\text{SO}_3^{2-}/\text{S}_2\text{O}_3^{2-}$  anions was neglected. In the first case, the concentration of  $\text{OH}^-$  is too  
299 weak for expecting a competition (pH ranging between 2.0 and 7.5). In the second case, this  
300 was checked experimentally: as shown in Fig. 3, the retention times of  $\text{I}^-$  and  $\text{Br}^-$  are similar in  
301 the presence or absence of the redox couple anions.

302 Fig. 3.



303

304 The determination of selectivity (exchange) coefficients requires modeling of the  
305 equilibrium at all stages of the column. In our dynamic system, the principle of “local  
306 equilibrium” was assumed, i.e. the rate of reactions was much more rapid than the rate of  
307 solute transport. It was checked for astatine considering the ultra traces concentrations of  
308 solute injected (about  $3.8 \times 10^8$  atoms corresponding to a concentration at the outlet of the  
309 column of  $10^{-13}$  mol L<sup>-1</sup>). The conditions were considered as ideal when the flow rate was  
310 below 500 μL min<sup>-1</sup>, no change of the astatine retention factor was observed with the flow rate  
311 (data not shown).

312 The influence of the ionic strength on the retention factor of Br<sup>-</sup>, I<sup>-</sup> and the astatine species  
313 is shown on Fig. 3. The log-log representation of the retention factor as a function of the ionic  
314 strength is linear. These experimental results are in agreement with the exchange process  
315 principle. Moreover, the modeling fairly reproduces the experimental data if we attribute one  
316 negative charge on astatine species. For illustration, the dashed line in Fig. 3 depicts the  
317 behaviour of a species with two negative charges. Hence, the experimental data confirm the  
318 existence of an anionic species with one negative charge.

319 The tendency for the relative selectivity coefficient of this species with respect to the  
320 others halides was next questioned. Berei [5], using the data of Roessler [14], showed a linear  
321 correlation within the halides series by plotting the retention volume as a function of the  
322 inverse ionic radius and stated it as an indirect proof of the existence of At<sup>-</sup>. The same trend  
323 should be found when plotting the relative selectivity coefficients as a function of the inverse  
324 ionic radius.

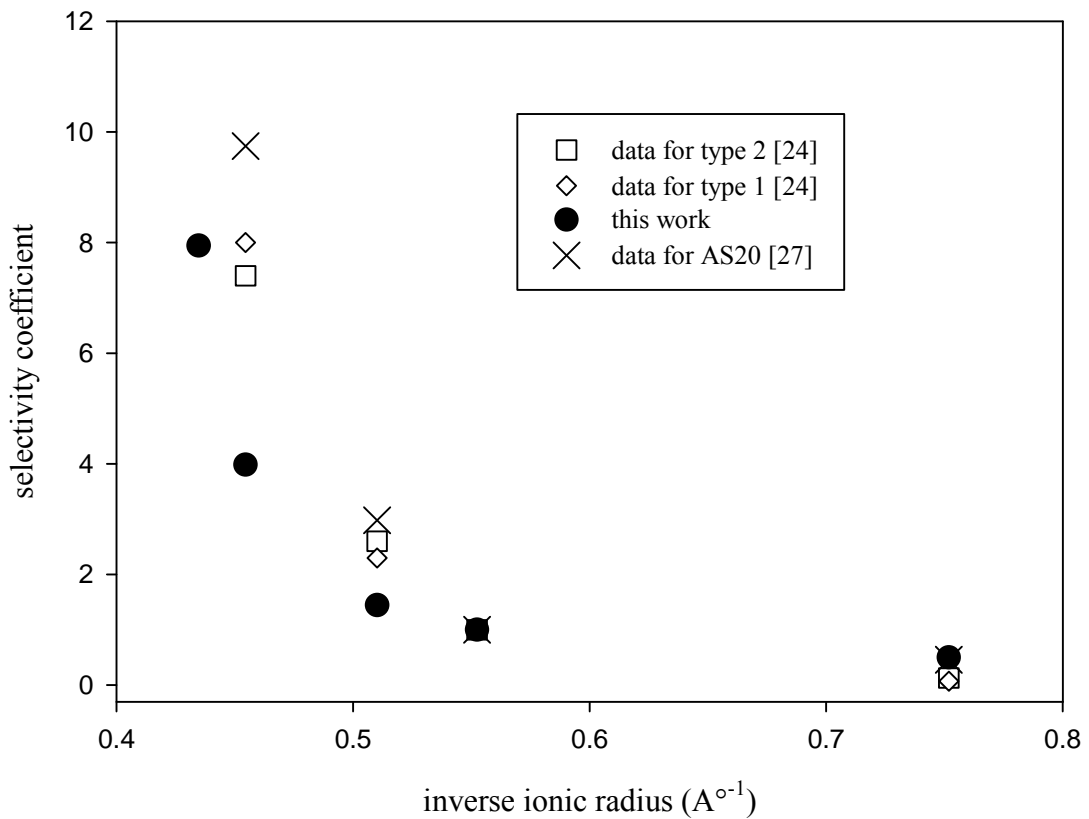
325 The reported coefficients (Fig. 4) were compared with  $K_{X/Cl}$  recalculated from published  
326 retention volumes obtained with polystyrene-divinylbenzene anion exchange resins with  
327 similar reactive sites [24] and those from retention factors specific for AS20 given by the



328 Virtual Column Separation Simulator 2 [27]. Note that values are given with respect to OH<sup>-</sup>  
 329 and the relative selectivity coefficients  $K_{X/Cl}$  were recalculated according to:

$$330 \quad K_{X/Cl} = \frac{K_{X/OH}}{K_{Cl/OH}}$$

331 Fig. 4. (5)



332  
 333 On the one hand, as shown in Fig. 4, the  $K_{X/Cl}$  values determined in the present work in  
 334 chloride medium are not identical with the  $K_{X/Cl}$  derived from hydroxide medium for AS20  
 335 and polystyrene-divinylbenzene anion exchangers. A correction of the activity coefficients for  
 336 the exchange species would be necessary, since the medium strongly influences the values of  
 337 selectivity coefficients [25]. Also, the differences may be explained by means of hydrophilic  
 338 character of resins: AS20 is highly hydrophilic while polystyrene-divinylbenzene resin is less  
 339 hydrophilic [28].

340 On the other hand, all plots of the relative selectivity coefficients as a function of the  
341 inverse ionic radius show an exponential-type curve. The empirical law of Berei [5] appears  
342 therefore to be not valid and could not demonstrate the existence of  $\text{At}^-$ . One can only  
343 conclude that (i) there is a coherence in the trend, i.e.  $K_{\text{At/Cl}} > K_{\text{I/Cl}} > K_{\text{Br/Cl}} > K_{\text{F/Cl}}$ , (ii) the  
344 species holds one negative charge, and (iii) the existence of an oxyanion is unlikely as it  
345 would not explain the data published in our previous work [21]. All results and the behaviour  
346 of astatine discussed in the introduction, provide an indirect proof of the existence of  $\text{At}^-$ .

347

348

### 349 3.2. *Astatine speciation in blood serum*

350

351

352 The behaviour of astatine in serum has been then investigated. The usual techniques of  
353 speciation of trace elements in biological environment were reviewed by Lobinski [29]. In the  
354 present case, the speciation of astatine in serum has been performed using HPAE- $\gamma$  system  
355 with the aims to simulate the equilibrium of astatine in blood serum and to monitor astatine  
356 species formed under physiological serum conditions.

357 In order to minimize external perturbation on the equilibrium in serum, the physiological-  
358 type mobile phase containing  $10^{-1}$  mol  $\text{L}^{-1}$  of NaCl,  $10^{-3}$  mol  $\text{L}^{-1}$  of PBS buffer and  $10^{-4}/10^{-3}$   
359 mol  $\text{L}^{-1}$  of  $\text{SO}_3^{2-}/\text{S}_2\text{O}_3^{2-}$  redox buffer has been prepared. The effect of the major serum  
360 components (transferrin, albumin, monovalent carbonate anion  $\text{HCO}_3^-$  and citrate) on  $\text{At}^-$   
361 elution was studied in model media before working with the biological medium. The  
362 investigated constituent is injected into the column and chloride competing agent is in mobile  
363 phase. The retention of a solute on the column is clearly related to the exchange reaction as  
364 described in equation (3) when  $\text{X}^- = \text{albumin, transferrin, PBS}$ . For mixture containing

365     astatine, the simple comparison of the retention with the  $\gamma$ -chromatograph from previous part  
366     of this study without any exchange evaluation has been done.

367

368

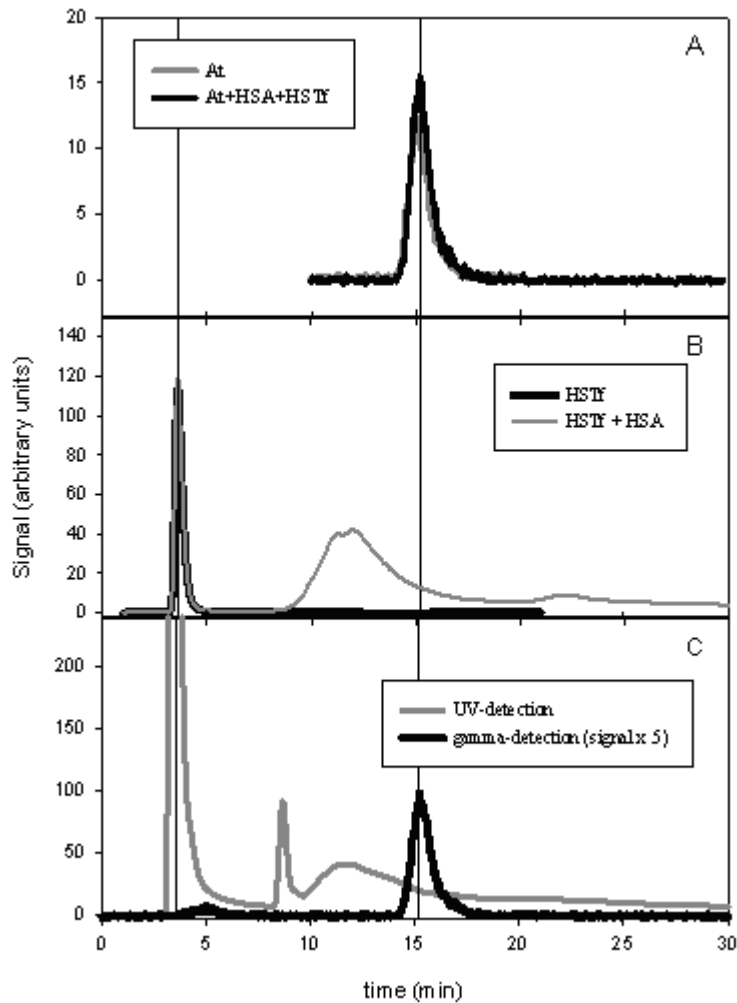
### 369     3.2.1. UV-characterization of major components in serum

370

371

372     The UV-chromatogram of the blood serum is given in Fig. 5. Three peaks at 2.5, 7.7 and  
373     10.5 min could be identified. The first peak eluted almost in the void volume (2.3 min) was  
374     identified as the peak of transferrin (Fig. 5B). The protein, dissolved in the physiological-type  
375     of eluent, was not retained on AS20 resin. Thus it is not expected to compete with astatine  
376     species for sorption sites. The broad peak at 10.3–11.0 min coincides with the elution of  
377     albumin which was dissolved in the synthetic physiological-type medium in the presence of  
378     transferrin (grey line in Fig. 5). The large full width at half maximum of the peak is explained  
379     by the presence of a mixture of the monomer and dimer of albumin. Whereas a better  
380     separation of monomer and dimer was obtained at a flow rate of  $500 \mu\text{L min}^{-1}$ , the resultant  
381     pressure exceeded the limit of the column. In synthetic media, 75-80% of the proteins were  
382     found at the exit of the column, while the restitution was lower (50-60 %) in the case of the  
383     serum. Obviously, the AS20 resin allows the resolution of both important metallo-proteins in  
384     “non-perturbing” conditions. Transferrin elutes nearly in the void volume while albumin is  
385     significantly retained on stationary support. The albumin retention has been quantitatively  
386     explained by an apparent selectivity coefficient  $K_{\text{Albumin/Cl}} = 0.15$  for exchange of  $\text{Cl}^-$  and one  
387     negative charge of albumin.

388     Fig. 5.



389

390 The experiments with the two main anionic low molecular weight components  
 391 (bicarbonate  $\text{HCO}_3^-$  and citrates  $\text{C}_3\text{H}_5\text{O}(\text{COO})_3^{3-}$ ) did not allow us to identify the peak eluted  
 392 at 7.7 min. Considering the complexity of the serum, this may be associated to the presence of  
 393 another low molecular weight molecule with high absorption extinction coefficient but  
 394 present in low amount. Therefore, it was not considered as a probable interfering species in a  
 395 first assumption. No further experiments were done for identifying it.

396

397

### 398 3.2.2. Characterization of astatine in serum

399

400

401 The  $At^-$  peak in the physiological-type medium was initially expected from modeling at  
402 the retention time of 15.3 min with a retention factor of 8.6, considering the previously  
403 determined selective coefficients and experimental conditions (electrolyte composition,  $\mu$ , pH  
404 and potential). The peak has appeared on the gamma chromatogram (Fig. 5) at the retention  
405 time of 15.3 min with a retention factor of 5.4 and a restored yield of 100%.

406 The damage of the resin over time leading to a decrease in the number of sites was  
407 therefore considered. The regular column tests done with iodide (see 2. Experimental section)  
408 have given a retention factor of 3.3, instead of 3.7 for a new column. This shift quantitatively  
409 explains 10% of decrease in retention sites number. This may result from a damage of the  
410 resin through the irradiation of alpha particles which are highly energetic. The model  
411 parameterization was changed accordingly for the further data evaluation.

412 However, the decrease of 10% sorption capacity of the resin can only partially explain the  
413 astatine shift because the retention factor would lower from 8.6 to 7.8. Complementary  
414 experiments with  $I^-$  under physiological type-conditions (in presence of PBS) were done. A  
415 decrease in retention factor is observed as compared to the one determined with  $0.1 \text{ mol L}^{-1}$   
416 NaCl as eluent (2.6 instead of 3.3). This peak shift has evidenced that the PBS buffer compete  
417 with  $X^-$  for sorption sites. In agreement with this assumption, the experimentally determined  
418 retention factors of  $I^-$  (3.3) and  $At^-$  (5.4) can truly be predicted using the previously  
419 determined coefficients  $K_{At/Cl}$  and  $K_{I/Cl}$  and including  $\log K_{PBS/Cl} = 1.7 \pm 0.1$ .

420 Transferrin and especially albumin represent the main potential competing agents in the  
421 blood medium. However, as Fig. 5A shows, no competition has occurred with proteins at the  
422 concentration encountered in the blood serum: in the presence and absence of proteins, the  
423 retention volumes of  $At^-$  are identical. This was also predicted using previously determined  
424 selectivity coefficients  $K_{Albumin/Cl}$ ,  $K_{At/Cl}$  and  $K_{PBS/Cl}$ . A similar result was obtained when  
425 carbonates and citrate ions were added to astatine solutions (data not shown). These results

426 show that  $\text{Cl}^-$  and phosphates present in the eluent exclusively govern the competition and that  
427 no interaction between  $\text{At}^-$  and major serum components occurs.

428 Astatine in presence of serum has given the peak at the same retention time (15.3 min)  
429 than the one observed in the physiological-type medium (Fig. 5A and Fig. 5C), and was  
430 restored more than 75%. This result can be seen as a genuine proof of the existence of  $\text{At}^-$  in  
431 the blood serum. The species was however restored at a yield slightly lower than those found  
432 with the physiological-type media. The presence of an additional cationic or neutral astatine  
433 species in weak amount strongly retained on the tubing of the HPAEC device cannot be  
434 excluded.

435

436

#### 437 **4. CONCLUSION**

438

439

440 The usefulness of HPAEC- $\gamma$  to get information regarding astatine speciation in simple  
441 and synthetic media, provided that a careful quantitative analysis is done, has been  
442 established. We report the first analytical result characterizing  $\text{At}^-$ : the species is anionic,  
443 holds one charge and its behavior is coherent in the halide series. A selectivity coefficient  
444  $K_{\text{At/Cl}}$  is given for the studied column. The methodology was successfully applied to  
445 biological medium. The resin used appears useful to separate the two important metallo  
446 proteins. Similar results with astatine were obtained in physiological-type and blood serum  
447 media; this indicates no interaction between astatine and serum components. In reducing  
448 conditions, astatine mainly exists as  $\text{At}^-$  in the blood serum. This is in agreement with in-vivo  
449 data found in the literature, i.e. astatide is attracted to the thyroid as  $\text{I}^-$  is [30]. The  
450 methodology is an alternative to the thin layer chromatography generally used for the in vitro

451 stability assessment of  $^{211}\text{At}$ -labelled molecules. Based on our results, the appearance of a  
452 peak corresponding to a retention factor of 5.3 would indicate the presence of astatide  
453 released from radio-labelled molecule, i.e. the binding between  $^{211}\text{At}$  and the carrier molecule  
454 in the sample incubated in the blood serum is not enough strong to compete with the  
455 formation of the thermodynamically stable astatide species in blood serum.

456

457

#### 458 **ACKNOWLEDGEMENT**

459

460

461 The authors would like to thank the “Agence Nationale de la Recherche” (ANR,  
462 JCJC06\_137852 and ANR-10-BLANC-0807), the “Région Pays de la Loire” (NUCSAN  
463 project and the grant allocated to Julie Champion), the scientific committee of the FR CNRS  
464 3173 “GRIM3” and the European Commission (TARCC project) for financial support. The  
465 authors are also grateful to CEMTHI team, especially to Isidro Da Silva, for the production of  
466  $^{211}\text{At}$ . We would like to address special thanks to Prof. Alain Faivre-Chauvet for providing  
467  $^{131}\text{I}$  and to Prof. Geerd-J. Meyer for fruitful discussion. Also, we thank DIONEX for having  
468 given us the data from the Virtual Column program and Anne-Marie Compiano to have read  
469 again the article.

470

471  
472 **FIGURE CAPTIONS**

473

474

475 Fig. 1. Parameters used for the simulation (1D dimension).

476

477 Fig. 2. Effect of the methanol content in the injected sample (in weigh percent) on the elution  
478 profile of astatine at  $350 \mu\text{L min}^{-1}$ ; eluent at pH 2 contains  $0.1 \text{ mol L}^{-1}$  of NaCl,  $10^{-2} \text{ mol L}^{-1}$   
479 of HCl, and  $10^{-4}/10^{-3} \text{ mol L}^{-1}$  of  $\text{SO}_3^{2-}/\text{S}_2\text{O}_3^{2-}$ .

480

481 Fig. 3. HPAEC results for  $\text{At}^-$  (circles),  $\text{I}^-$  (squares) and,  $\text{Br}^-$  (triangles); the flow rate was  
482 fixed between  $350$  and  $450 \mu\text{L min}^{-1}$ . Filled symbols:  $0.1 \text{ mol L}^{-1}$  NaCl; open symbols:  $10^{-2}$   
483  $\text{mol L}^{-1}$  of HCl,  $10^{-4}/10^{-3} \text{ mol L}^{-1}$  of  $\text{SO}_3^{2-}/\text{S}_2\text{O}_3^{2-}$  and  $10^{-1} \text{ mol L}^{-1}$  of NaCl. The lines are  
484 calculated with  $\log K_{X/Cl}$  values of 0.16, 0.58 and 0.90 for  $\text{Br}^-$ ,  $\text{I}^-$  and  $\text{At}^-$ , respectively. The  
485 dashed line represents a prediction considering that astatine species holds two negative  
486 charge.

487

488 Fig. 4. Variation of relative exchange selectivity coefficients for quaternary ammonium ions  
489 exchange resins as a function of the inverse ionic radii for the halides series. The filled and  
490 open symbols depict the data measured in this work and the published one [27] found for a  
491 similar type of resin, respectively. The selectivity coefficient for  $\text{F}^-$  was deduced from an  
492 experiment giving an elution time of 8 min (eluent:  $5 \times 10^{-2} \text{ mol L}^{-1}$  NaCl; flow rate:  $200 \mu\text{L}$   
493  $\text{min}^{-1}$ ).

494

495 Fig. 5. Speciation of astatine in human serum. (A)  $\gamma$ -chromatogram of astatine in the  
496 presence or absence of transferrin and albumin proteins (signal multiplied by a factor of 5 to





501 **REFERENCES**

502

503

- 504 1. D. R. Fisher, *Curr. Radiopharm.* 1 (2008) 127–134.
- 505 2. D. S. Wilbur, *Curr. Radiopharm.* 3 (2008) 144–176.
- 506 3. G. Vaidyanathan, M. R. Zalutsky, *Curr. Radiopharm.* 1 (2008) 177–196.
- 507 4. S. Lindegren, S. Frost, T. Back, E. Haglund, J. Elgqvist and H. Jensen, *J. Nucl. Med.*  
508 49 (2008) 1537–1545.
- 509 5. K. Berei, L. Vasaros, *Astatine Compounds*, 8<sup>th</sup> ed., Springer-Verlag, Berlin, 1985.
- 510 6. K. Berei, L. Vasaros, in: S. Patai and Z. Rappoport (Eds.), *The chemistry of halides,*  
511 *pseudo-halides and azides*, John Wiley & Sons Ltd., New York, 1995, pp. 787–819.
- 512 7. D. S. Wilbur, M.-K. Chyan, D. K. Hamlin and M. A. Perry, *Bioconjugate Chem.* 20  
513 (2009) 591–602.
- 514 8. T.C. Richardson, *Int. J. Appl. Rad. Instrum. B* 13 (1986) 583–584.
- 515 9. G. L. Johnson, R. F. Leininger and E. Segre, *J. Chem. Phys.* 17 (1949) 1–10.
- 516 10. V. D. Nefedov, Y. V. Norseev, M. A. Toropova and V. A. Khalkin, *Russ. Chem. Rev.*  
517 2 (1968) 87–98.
- 518 11. E. H. Appelman, E. N. Sloth and M. H. Studier, *Inorg. Chem.* 5 (1966) 766–769.
- 519 12. A. Cavallero and K. Rossler, *Radiochim. Acta* 47 (1989) 113–117.
- 520 13. Meyer, *Chromatographie trägerfreier anorganischer Formen von Jod-123 und Astat-*  
521 *211 und ihre Verwendung zur Halogenierung von Uracil and Desoxyuridin*, Berichte  
522 Nr.1076, Kernforschungsanlage Jülich, Jülich, 1974.
- 523 14. K. Roessler, W. Tornau and G. Stoecklin, *J. Radioanal. Chem.* 21 (1974) 199–209.
- 524 15. R. Dreyer, I. Dreyer, F. Rosch and G. J. Beyer, *Radiochem. Radioanal. Lett.* 54 (1982)  
525 165–175.
- 526 16. D. L. Parkhurst, C. A. J. Appelo, *User's guide to phreeqc—a computer program for*  
527 *speciation, batch-reaction, one-dimensional transport, and inverse geochemical*  
528 *calculations*, USGS Report No. 99–4259, 1999.
- 529 17. E. Ansoborlo, O. Prat, P. Moisy, C. Den Auwer, P. Guilbaud, M. VCarriere, B.  
530 Gouget, J. Duffield, D. Doizi, T. Vercouter, C. Moulin, V. Moulin, *Biochimie* 88  
531 (2006) 1605–1618.
- 532 18. C. Alliot, M. Chérel, J. Barbet, T. Sauvage, G. Montavon, *Radiochim. Acta* 97 (2009)  
533 161–165.
- 534 19. S. Lindegren, T. Back, H. J. Jensen, *Appl. Radiat. Isot.* 55 (2001) 157–160.
- 535 20. H. Sun, K. Y. Szeto, *J. Inorg. Biochem.* 94 (2003) 114–120.
- 536 21. J. Champion, C. Alliot, E. Renault, B. M. Mokili, M. Chérel, N. Galland and G.  
537 Montavon, *J. Phys. Chem. A* 114 (2010) 576–582.
- 538 22. C. W. Davies, *Ion association*, Butterworths, Washington D.C., 1962.
- 539 23. G. L. Gaines, H. C. Thomas, *J. Chem. Phys.* 21 (1953) 714–718.
- 540 24. F. de Dardel, *Techniques de l'ingénieur*, J2 783-782-716 (1998) 1–16.
- 541 25. B. Trémillon, *Les séparations par les résines échangeuses d'ions*, Gauthier-Villars,  
542 Paris, 1965.
- 543 26. J. Champion, C. Alliot, S. Huclier, D. Deniaud, Z. Asfari, G. Montavon, *Inorg. Chim.*  
544 *Acta* 362 (2009) 2654–2661.
- 545 27. J. E. Madden, M. J. Shaw, G. W. Dicoski, N. Avdalovic, P. R. Haddad, *Anal. Chem.*  
546 74 (2002) 6023–6230.
- 547 28. C. Liang, C. A. Lucy, *J. Chromatogr. A* 1217 (2010) 8154–8160.
- 548 29. R. Lobinski, C. Moulin, R. Ortega, *Biochimie* 88 (2006) 1591–1604.
- 549 30. D. S. Wilbur, *Bioconjugate Chem.* 19 (2008) 158–170.

550  
551  
552  
553